Ocean Dynamics (2015) 65:989–1000
DOI 10.1007/s10236-015-0849-3

On the consistency of the drag between air and water in meteorological, hydrodynamic and wave models

Joana van Nieuwkoop[1] · **Peter Baas**[2] · **Sofia Caires**[1] · **Jacco Groeneweg**[1]

Received: 28 November 2014 / Accepted: 11 May 2015 / Published online: 28 May 2015

Abstract For the design, assessment and flood control of water defences, hydraulic loads in terms of water levels and wave conditions are required and often obtained from numerical models. For these hydraulic loads to be reliable, accurate atmospheric forcing is required. Waves and surges are typically forced by surface stress. However, in most cases, the input for these models consists of 10-m wind velocities that are internally converted to surface stress by applying a particular drag relation. This procedure generally leads to inconsistencies, since the hydrodynamic, wave and atmospheric models often apply different drag relations. By means of a case study, we explored the consequences of this inconsistency in the drag formulation for a North Sea storm wave and surge hindcast. This was done by forcing the hydrodynamic and wave models using both the 10-m wind velocity and the surface stress fields computed by the atmospheric model. Our study results show significant differences between the wave parameter values and water levels computed with surface stress input and 10-m wind velocity input. Our goal is not to assess different drag parameterizations but to raise awareness for this issue and to plea for the use of a consistent drag relation in meteorological and hydrodynamic/wave models. The consistent use of one drag formulation facilitates the identification of problems and the eventual improvement of the drag formulation. Furthermore, we suggest using the so-called pseudo-wind, which is a translation of the surface stress to the 10-m wind speed using a reference drag relation.

Keywords Wind drag · Hindcast · HARMONIE · SWAN · WAQUA

Responsible Editor: Pierre Garreau

This article is part of the Topical Collection on the *17th biennial workshop of the Joint Numerical Sea Modelling Group (JONSMOD) in Brussels, Belgium 12–14 May 2014*

✉ Joana van Nieuwkoop
Joana.vanNieuwkoop@deltares.nl

1 Deltares, Boussinesqweg 1, 2629 HV Delft, The Netherlands

2 KNMI, Utrechtseweg 297, 3731 GA De Bilt, The Netherlands

1 Introduction

A significant part of The Netherlands lies below sea level. Therefore, the Dutch flood protection system needs to be well designed and reliable to maintain safety and sustain economic development. To support these objectives, the quality of the Dutch flood defence system is assessed periodically. In the assessment, the strength of the flood defences is compared with the hydraulic load on the flood defences under normative conditions. The latter are called hydraulic boundary conditions and consist of a combination of water level and wave conditions.

In addition, waves and storm surges are operationally forecasted by the Dutch storm surge warning service (SVSD) to be prepared against floods during extreme events. During an extreme event, dikes will be monitored in the field to prevent them from breaching and measures can be taken for evacuation. Accurate forecasts at least 6 h ahead are also needed for proper closure of the movable storm surge barriers in the Eastern Scheldt and the New Waterway in The Netherlands.

To obtain reliable computed waves and surges, accurate atmospheric forcing is required to drive the hydrodynamic and wave models. One point of attention is the consistency of the wind drag between the atmospheric, the hydrodynamic and the wave models. Normally, the input for the numerical models consists of 10-m wind velocities that are internally converted to surface stress by applying a particular drag relation. However, the atmospheric model also uses a particular drag relation to determine the surface stress from the wind velocity at the lowest atmospheric level. This procedure generally leads to inconsistencies and errors, since the hydrodynamic, wave and atmospheric models often apply different drag relations. All the more as in storm surge models, the drag coefficient is often used as a tuning parameter.

Moreover, a large uncertainty exists in the magnitude of the drag coefficient. Often, a wind drag relation is assumed that depends only on the wind speed and increases with increasing wind speeds. This is the case for the often used *Charnock relation* (Charnock 1955). However, Babanin and Makin (2008) conclude that the drag coefficient is depending on many more factors, like sea state, effects of wind trends and gustiness. This means that a more accurate drag can only be determined if the atmospheric model is coupled with a wave model to enable a two-way interaction between surface winds and waves. This step has already been taken at the European Centre for Medium-Range Weather Forecasts (ECMWF), where this two-way coupling is achieved through the exchange of the Charnock parameter between the atmospheric model and the wave model WAM. Janssen et al. (2002) show that coupling the wind and waves improves the prediction of both wind velocities in the atmospheric boundary layer and wave parameter values. Muller et al. (2014) show that also the prediction of surges improves when a variable Charnock coefficient, depending on a statistical description of the sea state, is taken into account.

Another point of attention is that the drag coefficient decreases in measured wind profiles during extreme wind velocities (wind speeds larger than about 33 m/s), as was observed by Powell et al. (2003). By describing the impact of spray droplets on the atmospheric flow in the boundary layer, Makin (2004) was able to explain the observed reduction and to describe the drag coefficient during extreme wind speeds based on a resistance law of the sea surface. Makin's wind drag parameterization was tested by Vatvani et al. (2012) for the storm surge of two hurricane events, modelled in Delft3D. It was concluded that Makin's new drag parameterization is favourable above the traditional Charnock relation. Also, Zijlema et al. (2012) came up with a new wind drag parameterization with lower drag values than those of the Charnock relation for extreme wind speeds, which was implemented into the spectral wave model SWAN (Booij et al. 1999).

Zweers et al. (2011) studied how uncertainties in the magnitude of the drag coefficient translate into uncertainties in storm surges. They forced the hydrodynamic model WAQUA/DCSM (Gerritsen et al. 1995) directly with surface stresses, computed using the atmospheric model HIRLAM (http://hirlam.org/), applying the Charnock relation with different values of the Charnock parameter. They found that when the Charnock parameter in HIRLAM is changed, the relative increase in the stress is approximately 50 % of the relative increase in the drag coefficient during storm conditions. This is because for an increase in the drag coefficient, the weakening of the 10-m wind field reduces the increase in the stress considerably. This is advantageous, since possible errors in the surface drag are suppressed in the stress response. Subsequently, the relative change in storm surge at stations along the Dutch coast is approximately 36 % of the relative change in drag coefficient.

In this study, we go a bit further than Zweers et al. (2011) by studying also how the use of different drag relations affect the waves. More precisely, this study explores the consequences for waves and surges when the drag formulation is used inconsistently between models. This is done with a case study of the All Saints storm (30 October 2006 to 3 November 2006) over the North Sea, with special attention to the hydraulic conditions at the Dutch coast. This particular storm has been chosen because its hydraulic loads were very high, in particular for the northern parts of The Netherlands. According to the statistics of the Dutch meteorological institute KNMI, a storm of this magnitude occurs circa 14 times in 1000 years. One set of computations is done with the 10-m wind velocities from the atmospheric model and the default drag relations of the wave and surge models. A second set of computations is done with the surface stress from the atmospheric model directly forcing the wave and surge models. That way, no extra (or inconsistent with the atmospheric model) drag relation is applied in the wave and surge models. Subsequently, the wave and surge results of the two types of computations are compared. In addition, we discuss different ways in which the atmospheric forcing can be applied.

The outline of this paper is as follows: we start with discussing some basic concepts and formulas regarding to the air-sea interface in Section 2. Subsequently, in Section 3, a description is given of the atmospheric model, the hydrodynamic model and the wave model that were used in the storm hindcast. Special attention is paid to the drag formulations of each model. Section 4 presents a comparison of the wind input and also shows the results of the different wave and hydrodynamic model runs. Finally, in Section 5, the problem of an inconsistent drag relation is discussed and possible solutions for this problem are evaluated.

2 Basic concepts

In most cases, the hydrodynamic or wave models are driven by wind velocities, referenced at a 10-m height (U_{10}). The 10-m velocities are internally converted to surface stress by applying a particular drag relation to force the waves and surges. The surface stress (τ) is the momentum flux through the air-sea interface and is formulated as follows:

$$\tau = \rho_a C_d U_{10}^2 \quad (1)$$

Here, ρ_a is the air density and C_d is the drag coefficient.

As mentioned in Section 1, whereas the drag coefficient depends on both wind speed and wave state, it is usually computed solely as a function of the 10-m wind speed using the Charnock relation. Furthermore, there exists a large uncertainty associated with its determination for higher wind velocities, as measurements are sparse.

The use of the Charnock relation to compute C_d involves first the calculation of the aerodynamic roughness length (z_0):

$$z_0 = \alpha \frac{u_*^2}{g} \quad (2)$$

which can be complemented with viscous effects $0.11\nu/u_*$ for low wind speeds. Here, α is the Charnock parameter, u_* the friction velocity ($u_*=\sqrt{(\tau/\rho_a)}$), g the gravitational acceleration and ν the kinematic viscosity of air. Subsequently, the roughness length, z_0, is used to calculate the drag coefficient, assuming a logarithmic wind profile:

$$C_d = \left(\frac{u_*}{U_{10}}\right)^2 = \left(\frac{\kappa}{ln\left(\frac{10}{z_0}\right)}\right)^2 \quad (3)$$

with a Von Karman constant κ of 0.4.

3 Models

3.1 Introduction

A case study was set up with the atmospheric model HARMONIE, the hydrodynamic model WAQUA and the wave model SWAN to study the effects of the inconsistent use of drag. In this section, the different models are described and special attention is given to the drag formulations of each of the models. In our case study that is described in Section 4, the HARMONIE model was run to compute the 10-m wind velocities and the surface stress. The HARMONIE wind velocities or stresses were used to force the WAQUA model. The main output variable of this model is the still water level (SWL), the level that the sea surface (at a given point and time) would assume in the absence of wind waves. SWLs are influenced by astronomical and meteorological effects. The WAQUA model was run with and without atmospheric forcing and two variables have been computed from the results:

- The surge, S, defined as the synchronous difference between the still water level computed in the run with atmospheric forcing and the tide computed in the run with no atmospheric forcing; and
- The skew surge, h_s, defined in a tidal cycle as the difference between the highest (lowest) SWL from the run with atmospheric forcing and highest (lowest) level due to astronomical tide in the run with no atmospheric forcing.

The SWAN model was forced with HARMONIE wind speeds or stresses. The computed significant wave height, H_{m0}, was considered for further analyses.

3.2 HARMONIE

HARMONIE (*H*IRLAM *A*LADIN *R*esearch *on M*esoscale *O*perational *N*WP *i*n *E*uromed) is the operational numerical weather prediction model of the Dutch meteorological institute KNMI. It is a limited-area model that has been developed in a consortium involving many European countries. HARMONIE is the successor of the hydrostatic HIRLAM and the ALADIN models. Major differences with relation to these models are that HARMONIE is intended to run on a very high resolution and that it is a so-called non-hydrostatic model. The latter means that instead of employing the hydrostatic approximation, which often breaks down in severe weather events, the vertical momentum equation is solved explicitly. More details on HARMONIE (also referred to as AROME) are given by Seity et al. (2011) (see also the documentation on www.hirlam.org). Here, we used HARMONIE CY37h1.1 that was released on 13 June 2012.

HARMONIE runs on a regular grid with a grid spacing of 2.5 km. HARMONIE is a limited-area model, meaning that it covers only a part of the globe. A domain size of 500×500 grid point (1250×1250 km), centred at 54° N 2° E, was used (see Fig. 1). Because HARMONIE is run in a limited area, information on the state of the atmosphere on the lateral boundary conditions is required. For this, we use data from the ERA-Interim reanalysis dataset from the ECMWF (see http://www.ecmwf.int/en/research/climate-reanalysis/era-interim, Dee et al. 2011). More details on the model settings and validation of its results can be found in Baas et al. (2015).

HARMONIE makes a distinction between 'sea' and 'inland water bodies' for the surface drag over water. The interaction between the sea surface and the atmosphere is calculated by the Exchange Coefficients from Unified Multi-campaigns Estimates (ECUME) module. ECUME is a bulk iterative parameterization developed in order to obtain optimal exchange coefficients for a wide range of atmospheric and oceanic conditions. In ECUME, the neutral drag coefficients are directly estimated from the 10-m wind velocity by empirical formulae. These are based on the ALBATROS database that consists of data from five flux measurement campaigns (Weill et al. 2003). It should be noted that the influence of the waves on the wind drag was not taken into account in the

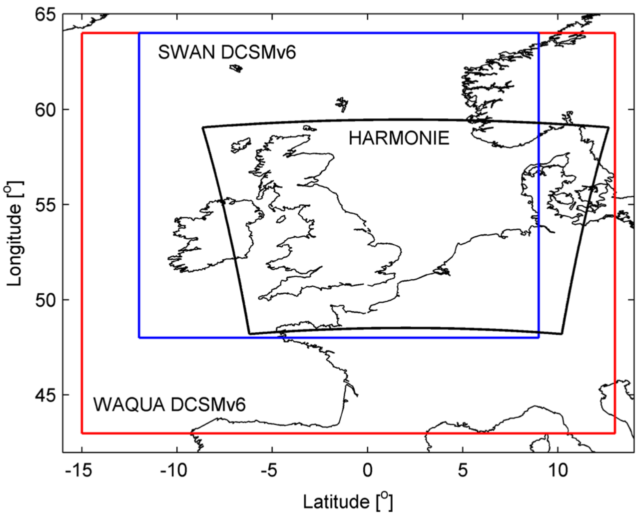

Fig. 1 HARMONIE domain, WAQUA DCSMv6 domain and SWAN DCSMv6 domain

parameterization of ECUME. For high wind speeds, the ECUME formulation is roughly equivalent to a Charnock formulation with α=0.020 (see Fig. 2), but values occur that are closer to α=0.032. Contrasting to the Charnock relation, the ECUME relation predicts a decrease in wind drag for wind speeds larger than ca. 30 m/s. Over lakes and rivers, a Charnock formulation with a parameter of α=0.015 is used in HARMONIE. The air density in HARMONIE is variable and is computed in HARMONIE using the gas law and depends, thus, on the temperature.

3.3 Simulation system for water movement and quality (WAQUA)

WAQUA is a hydrodynamic and water quality simulation system, used for modelling 2D (horizontal) schematizations of water systems. WAQUA is a module of SImulatie MOdellen NAtte (SIMONA), a framework for hydrodynamic modelling of free-surface water systems, based on the finite difference method. It is used by the Dutch public works authority (Rijkswaterstaat) in and around The Netherlands. WAQUA is able to compute water levels, currents and particle transport in open water.

A schematization of WAQUA is the Dutch Continental Shelf Model (DCSM), which is used by the Dutch Storm Surge Warning Service to provide forecasts of the Dutch waters. In this study, version 6 of the DCSM model (DCSMv6, Zijl et al. 2013) has been used. An overview of the DCSMv6 hydrodynamic model domain is shown in Fig. 1. The model's spherical grid has a uniform cell size of 1.5′ (1°/40°) in the east-west direction and 1.0′ (1°/60°) in the north-south direction. This corresponds to a grid cell size of about 2 by 2 km.

At the open northern, western and southern sides of the model's domain, water level boundaries are defined. The water levels imposed at the open boundaries can be split into a tidal and non-tidal part. To account for the effect of bottom friction, a spatially varying roughness field determined in the model calibration is applied. The minimum bottom roughness applied is 0.012 s/m$^{1/3}$.

In WAQUA, three possibilities exist to describe the drag coefficient. The most simple way is to use a constant drag coefficient. The second way is to formulate the drag by means of two drag coefficients: C_{dA} and C_{dB} in combination with two wind speed values U_{A} and U_{B}. Below U_{A}, the drag is C_{dA}; between U_{A} and U_{B}, the drag is linearly interpolated between C_{dA} and C_{dB}; and above U_{B}, the drag is C_{dB}. The last option is to use the Charnock relation to describe the drag. WAQUA's default Charnock parameter is 0.032. This is the value which the Dutch meteorological institute advised the Dutch operational flood forecast service to use in shallow waters in general and above the North Sea in particular. However, the DCSMv6 model uses a Charnock parameter of 0.025, which is consistent with the value used in the atmospheric model HIRLAM. By default, an air density ρ_{a} of 1.205 kg/m^3 is used. In most cases, this air density will not be identical with the air density used in HARMONIE.

In the more recent versions of WAQUA, it is possible to force WAQUA directly with the surface stress. In that way, no drag relation needs to be specified in the WAQUA model. Zweers et al. (2011) used surface stress input in WAQUA to study the influence of inaccuracies in the wind drag on the skewed surge.

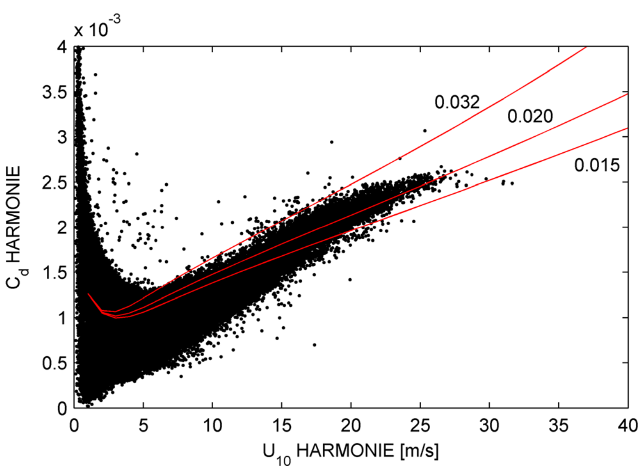

Fig. 2 ECUME relation used by HARMONIE over sea. The *dots* present the wind drag C_{d} calculated with ECUME against the wind velocity U_{10} for a hindcast period of 35 years at locations in the North Sea. The *solid lines* indicate a Charnock relation with parameters α of 0.015, 0.020 and 0.032

3.4 SWAN

The spectral wave model SWAN (Simulating WAves Nearshore) is a third-generation wave action model. SWAN accounts for wave propagation, depth and current-induced refraction and represents processes that generate, dissipate or redistribute wave energy. These include the deep water processes of wind input, whitecapping dissipation and quadruplet non-linear interaction and the shallow water processes of bottom friction dissipation, depth-induced breaking and triad wave-wave interactions.

A schematization of the DCSM also exists for SWAN to provide wave forecasts for the Dutch waters. The DCSM-SWAN grid is regular and its domain is slightly smaller than the DCSMv6 WAQUA domain (see Fig. 1). It has a grid resolution of approximately 3.6 km×3.6 km. The wave boundary conditions are obtained from the operational ECMWF wave model. Here, the wave model WAM is coupled with the ECMWF atmospheric model (Janssen 2004). SWAN is run in non-stationary mode.

By default, the wind drag coefficient is computed in SWAN according to the Wu (1982) formulation, supplemented with an imposed lower limit (Zijlema et al. 2012):

$$C_{\mathrm{d}} = \begin{cases} 1.2875 \times 10^{-3} \text{ for } U_{10} < 7.5 \text{ m/s}, \\ (0.8 + 0.065 U_{10}) \times 10^{-3} \text{ for } U_{10} \geq 7.5 \text{ m/s}. \end{cases} \quad (4)$$

Version 40.91 now also includes an additional drag formulation (see Zijlema et al. 2012), as mentioned in Section 1. It is a second-order polynomial fit through different datasets of drag measurements (up to 60 m/s):

$$C_{\mathrm{d}} = \left(0.55 + 2.97\frac{U_{10}}{U_{\mathrm{ref}}} - 1.49\left(\frac{U_{10}}{U_{\mathrm{ref}}}\right)^2\right) \times 10^{-3} \quad (5)$$

where U_{ref} is a reference wind of 31.5 m/s. This drag formulation provides a more realistic relation for extreme winds than when using the Wu relation. However, when using this formulation in combination with wind from an atmospheric model, still inconsistencies occur, as the drag formulations used by SWAN and the atmospheric model differ. The default setting for air density in SWAN is 1.28 kg/m^3, which also differs from the air density used in HARMONIE and WAQUA. This is another inconsistency.

Until this study, there was no option to input surface stress directly into SWAN. For this study, we have implemented this option in SWAN version 40.91.

4 Case study

4.1 Introduction

The All Saints storm was chosen as a case study. On 31 October 2006, a storm depression moved eastward over the northern North Sea. At the west side of the depression, a strong northwesterly flow developed over the entire North Sea. In the north of The Netherlands, the peak of the storm, associated with the passage of a sharp trough, occurred at 6 UTC in 1 November with hourly averaged wind speeds of more than 20 m/s (Fig. 3). The prolonged northwesterly wind field and the long fetch over the North Sea led to record-breaking surge and SWL levels in Delfzijl. The All Saints storm is also referred to as the 'Horses storm', because 227 horses were isolated due to flood in Marrum, 25 horses drowned and the rest were saved in a spectacular rescue operation.

This particular storm has been chosen because its hydraulic loads were very high, in particular for the northern parts of The Netherlands. According to the statistics of the Dutch meteorological institute KNMI, a storm of this magnitude occurs circa 14 times in 1000 years. Furthermore, the storm is very representative for The Netherlands, because of its northwesterly wind direction, which affects the whole Dutch coast.

The HARMONIE model was used to hindcast the period from 28 October to 3 November. The wind velocities and stresses computed by HARMONIE were used to force WAQUA and SWAN. Because the HARMONIE grid does not fully cover the WAQUA and SWAN grids (cf. Fig. 1), HIRLAM data were used to force the models in the regions not covered by the HARMONIE data. Furthermore, the period of 28 to 30 October is used for the spin-up of the WAQUA and SWAN models and is not considered in the analysis presented next. The analysis of the surge and wave response only focuses on a sub-region of the DCSM domains (cf. Fig. 3), with special attention to the Dutch coast.

4.2 Comparison of the drag relations

In order to explore the consequences for waves and surges when the drag formulation is used in its presently inconsistent way, two different sets of computations were done. Figure 4 shows the methodology for the first and second sets of computations.

The first set of computations (hereafter denoted as set 1) was done in the traditional way. U_{10}-wind velocities from the atmospheric model HARMONIE are used as input for the wave model SWAN and surge model WAQUA (see Fig. 4a). HARMONIE uses a drag coefficient, C_{d0}, derived from the ECUME drag relation. In WAQUA and SWAN, the U_{10}-wind velocities are internally converted to surface stresses (τ_{u1} for WAQUA and τ_{u2} for SWAN) using Eq. 1 with drag coefficients C_{d1} (WAQUA) and C_{d2} (SWAN) and constant air densities, which are unequal to the variable air density used in HARMONIE. C_{d1} is determined with the Charnock relation using Eqs. 2 and 3 with WAQUA's default value for α (α= 0.032). For SWAN, the Wu relation (see Eq. 4) is used to compute C_{d2}, which roughly compares to the Charnock relation with a parameter α=0.0185. As each of the three models uses a different drag relation, the result of these procedures is that the surface stresses that are used in WAQUA, SWAN and HARMONIE are all different.

Fig. 3 Spatial distribution of U_{10} in a sub-region of the DCSM domains—wind speeds and direction (*arrows*) during the peak of the storm at time 1 November 2006, 06:00 at K13. The water level stations (*circles*) and wave stations (*squares*) that were used in this study are marked

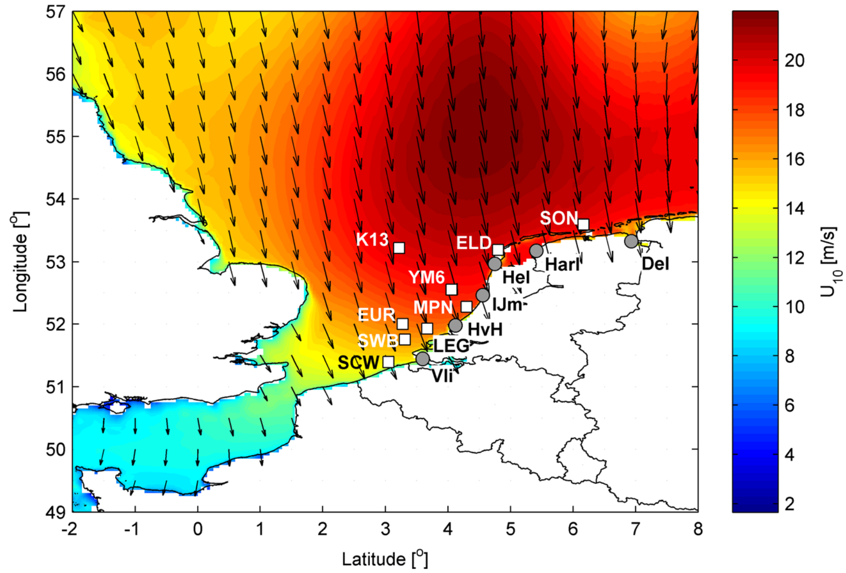

A second set of computations (hereafter denoted as set 2) was done with the surface stresses from the atmospheric model directly forcing WAQUA and SWAN (see Fig. 4b). Like in set 1, the HARMONIE surface stresses are based on the ECUME drag relation. However, as WAQUA and SWAN are forced directly by surface stresses (denoted by τ_τ), no extra drag relations have been applied in those models and the surface stresses τ and τ_τ are equal.

It should be noted that set 2 could also be modelled according to Fig. 5, with so-called pseudo wind input. Like in set 2, in this methodology, the surface stresses from HARMONIE are used. However, before the surface stresses are used as input for the hydrodynamic models, they are translated to the 10-m wind speed ($U_{10,\tau 1}$ for WAQUA and $U_{10,\tau 2}$ for SWAN) using a reference drag relation and a reference air density equal to the one used in the wave or flow models. In the case of WAQUA, we apply the Charnock relation (Eqs. 2 and 3), with α=0.032. For SWAN, we use the Wu relation (Eq. 4). Subsequently, this reference drag relation should be used in the model settings of WAQUA, respectively, SWAN. The results of the pseudo wind computations are the same as those of set 2. However, the interpretation of the wind fields is more intuitive than the stress fields. In the following paragraphs, use is made of the pseudo wind to compare the wind fields of set 1 and set 2.

In Fig. 6, the surface drag from the drag relations used in HARMONIE, WAQUA and SWAN is presented as a function of the U_{10}-wind velocity range of the All Saints storm. The drag coefficients from HARMONIE are calculated with Eq. 1 and the HARMONIE U_{10}, the surface stresses and an air

Fig. 4 **a** The methodology for set 1 computations. **b** The methodology for set 2 computations

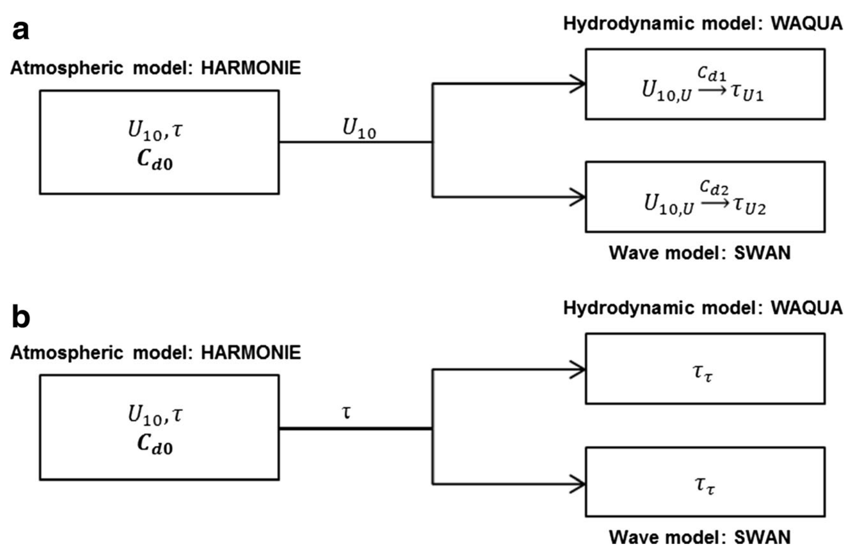

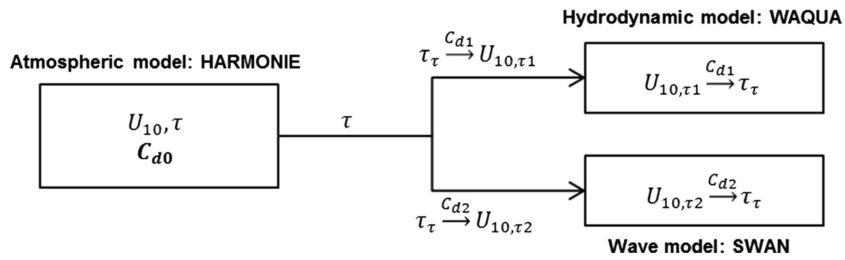

Fig. 5 Methodology for the pseudo wind input

density of 1.28 kg/m^3 for the duration of the All Saints storm. It can be seen that the wind drag in HARMONIE is lower than in WAQUA and SWAN for wind velocities smaller than approximately 15 m/s. For wind velocities higher than 15 m/s, the wind drag of SWAN is lower than the wind drag of HARMONIE. The wind drag in WAQUA is for all cases, except for wind speeds lower than 4 m/s, higher than in HARMONIE and SWAN.

We will study the consequences of these differences in wind drag between the models in the next sections. In Section 4.3, the surge from WAQUA of set 1 will be compared to that of set 2. And in Section 4.4, the waves from SWAN of set 1 will be compared to those of set 2.

4.3 Comparison of water levels

Figure 7 shows the comparison for the surge, S, between the set 1 and set 2 computations with WAQUA. In Fig. 7a, the spatial distribution of the surge of set 2 during the surge peak at Hoek van Holland is presented. Figure 7b shows the mean difference between set 1 and set 2, $<\delta S> = <S_U - S_\tau>$, over the period 30 November to 3 November; Fig. 7c the standard deviation σ; and

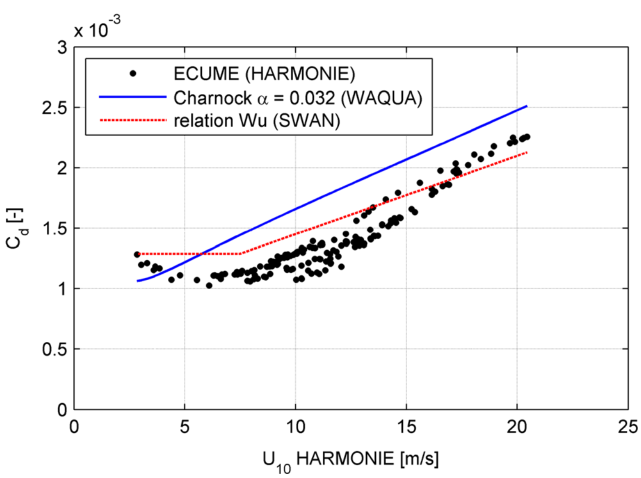

Fig. 6 A comparison of the drag relation of ECUME used in HARMONIE (*dots*), the Charnock relation with α 0.032 of WAQUA (*solid line*) and the Wu relation used in SWAN (*dashed line*) at K13 for the November 2006 storm

Fig. 7d the maximum difference between the surge computed with set 1, S_U, and the surge computed with set 2, S_τ. Mean differences in the order of several centimetres are observed, especially near the Dutch coast, with maxima of 12 to 18 cm. The surge S_U is higher than the surge S_τ as expected given that the drag coefficient used by default in WAQUA is generally higher than the drag coefficient used in HARMONIE (cf. Fig. 6 and Eq. 1).

In Fig. 8, the time series of the wind and surge evolution at Hoek van Holland are presented for the days around the peak of the storm. Figure 8a shows both the U_{10}-wind speed and the storm surge time series for set 1 and set 2. The observed surge is shown as well to illustrate the differences between the observation and the model computations of set 1 and set 2. Absolute differences in surge between set 1 and set 2 up to 12 cm are observed in Fig. 8b, whereas the absolute differences in wind velocity are in the order of 1 m/s. Figure 8c shows the relative differences in surge ($\delta S/S_\tau$), compared to the relative differences in U_{10}-wind speeds ($\delta U_{10}/U_{10,\tau}$) and drag coefficients ($\delta C_d/C_{d,\tau}$) between set 1 and set 2. In the period that the wind speeds are higher than 15 m/s (the period between about 1 and 8 a.m. in 1 November), the relative differences of U_{10} and S are both between 4 and 6 %, whereas the relative difference of C_d is between 10 and 12 %. In the period prior to the storm peak, the relative surge is about two times the relative U_{10}. In these conditions, the surge is probably proportional to the wind speed squared, so that the following relation holds: $\delta S/S_\tau \sim 2\delta U_{10}/U_{10,\tau}$.

The relation between the relative difference in surge and the relative difference in drag is further illustrated in Figs. 9 and 10. For the six coastal stations Vlissingen (Vli), Hoek van Holland (HvH), IJmuiden (IJm), Den Helder (Hel), Harlingen (Harl) and Delfzijl (Del) (see Fig. 3), the relative surge and skew surge, as defined in Section 3.1, were calculated from the results of the set 1 and set 2 computations. Figure 9 presents $\delta S/S_\tau$ against $\delta C_d/C_{d,\tau}$ for all instances where U_{10}>10 m/s and S>0.1 m (dots), and for all instances where U_{10}>15 m/s and S>0.1 m (star markers). A clear relation is observed between the relative drag and the relative surge; the larger the difference in drag, the larger the difference in surge. For the higher wind velocities (U_{10}>15 m/s),

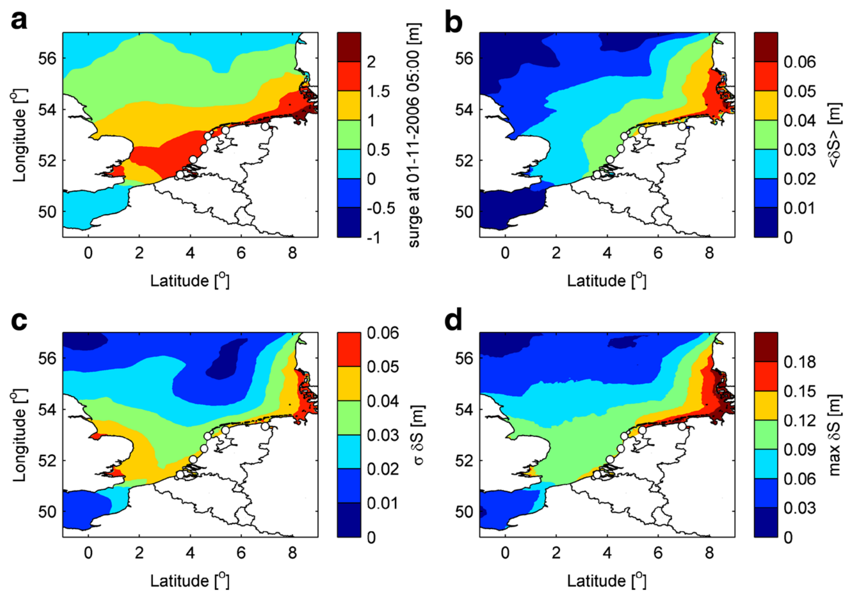

Fig. 7 **a** The surge distribution for set 2 at the surge peak at Hoek van Holland on 1 November 2006, 05:00. **b** Mean difference of the surge of set 1 and set 2 $<\delta S>=<S_U-S_\tau>$. **c** The standard deviation σ for $\delta S=S_U-S_\tau$. **d** Maximum difference for $\delta S=S_U-S_\tau$

$\delta C_d/C_{d,\tau}$ is relatively low (< 0.3), as can be seen also in Fig. 6. The resulting response in $\delta S/S_\tau$ is smaller than for the wind velocities $10<U_{10}<15$ m/s.

Figure 10 shows the response of $\delta h_s/h_{s,\tau}$ against $\delta C_d/C_{d,\tau}$ for all instances where the skew surge is higher than 1 m. A similar figure can be found in Zweers et al. (2011), where they show the response in $\delta h_s/h_{s,\tau}$ for different $C_d/C_{d,\tau}$ based on seven runs with HIRLAM with different values of the Charnock parameter, relative to a default run and four different storm periods, including the November 2006 storm. In this study, contrasting to Zweers et al. (2011), the variation in $C_d/C_{d,\tau}$ is due to variations in the ECUME relation relative to WAQUA's Charnock relation with α of 0.032. Furthermore, the results are based on only one storm period. However, Zweers et al. (2011) state that results of individual storms were very similar, so the results should still be comparable.

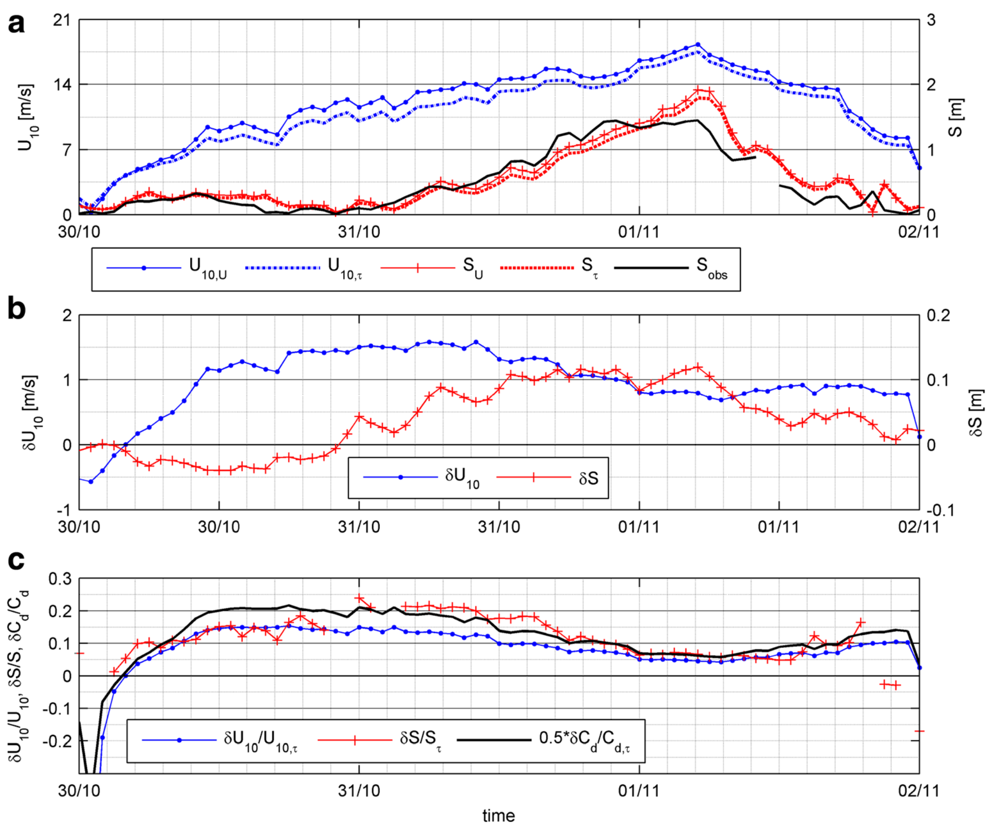

Fig. 8 Difference in surge S compared to difference in wind velocity and wind drag at Hoek van Holland. **a** The computed U_{10} and S for set 1 and set 2 and the observed S. **b** The absolute difference between set 1 and set 2 for U_{10} and S. **c** The relative difference between set 1 and set 2 for U_{10}, S and C_d

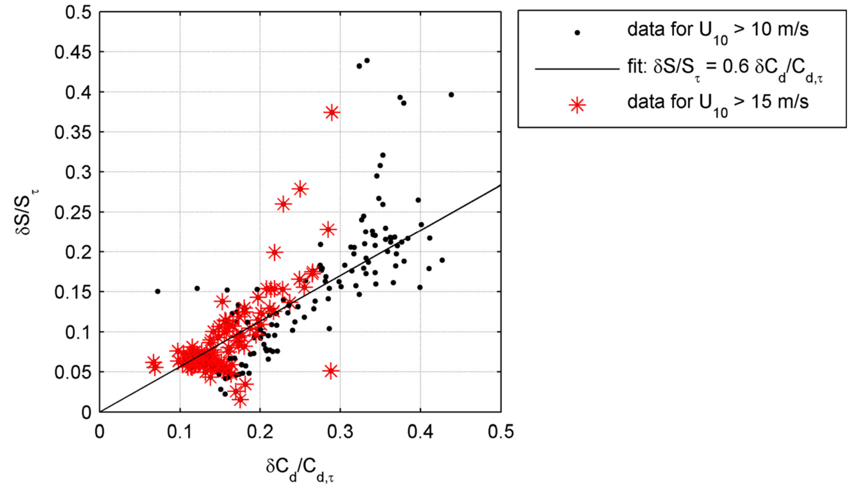

Fig. 9 The response of WAQUA in relative surge ($\delta S/S_\tau$) is shown against the relative difference in drag coefficients $\delta C_d/C_{d,\tau}$ between HARMONIE and WAQUA for all instances where U_{10}>10 m/s and the surge S> 0.1 m for the six coastal stations Vli, HvH, IJm, Hel, Harl and Del

The best fit for Zweers et al. (2011) is $\langle \frac{\delta h_s}{h_s} \rangle = 0.36 \langle \frac{\delta C_d}{C_d} \rangle$. Here, < > indicates that an average value is used over the entire domain during the entire model run. In this study, a best fit was found of

$$\frac{\delta h_s}{h_{s,\tau}} = 0.4 \frac{\delta C_d}{C_{d,\tau}}.$$

The results are very comparable, given the differences between this study and the study of Zweers et al. (2011).

4.4 Comparison of significant wave height

Figure 11 shows the comparison for the significant wave height, H_{m0}, between the set 1 and set 2 computations with SWAN. In Fig. 11a the spatial distribution of H_{m0} for set 2 during the significant wave height peak on 1 November 2006, 06:00 is presented. Figure 11b shows the mean difference, $<\delta H_{m0}> = <H_{m0,U} - H_{m0,\tau}>$ over the period 30 October to 3 November, Fig. 11c the standard deviation σ and Fig. 11d the maximum difference between H_{m0} computed with set 1, $H_{m0,U}$, and H_{m0} computed with set 2, $H_{m0,\tau}$. Mean differences up to 10 cm are observed, with maxima of 40 to 50 cm.

In Fig. 12, the time series of the wind velocity U_{10} and significant wave height evolution are presented for K13. Figure 12a shows both the U_{10}-wind velocity and the significant wave height time series for set 1 and set 2. The observed significant wave height is shown as well to illustrate that the differences between set 1 and set 2 are smaller than the differences between model and observation. Absolute differences in significant wave height of set 1 and set 2 up to plus and minus 30 cm are observed in Fig. 12b, whereas the absolute differences in wind velocity are between 1 and −0.5 m/s. Figure 12c shows the relative differences in significant wave height ($\delta H_{m0}/H_{m0,\tau}$), compared to the relative differences in U_{10}-wind velocities ($\delta U_{10}/U_{10,\tau}$) and drag coefficients ($\delta C_d/C_{d,\tau}$) for set 1 and set 2. In the period around the storm peak, the relative differences of U_{10} and H_{m0} are both between −2 and −4 %, whereas the relative difference of C_d is between −6 and −7 %. However, the relative differences are larger prior to the storm peak, with $\delta U_{10}/U_{10,\tau}$ up to 10 %, $\delta C_d/C_{d,\tau}$ up to 25 % and $\delta H_{m0}/H_{m0,\tau}$ up to 15 %. As seen for the storm surge, $\delta H_{m0}/H_{m0,\tau}$ is approximately two times $\delta U_{10}/U_{10,\tau}$.

The relation between $\delta H_{m0}/H_{m0,\tau}$, $\delta U_{10}/U_{10,\tau}$ and $\delta C_d/C_{d,\tau}$ has been studied further in Figs. 13 and 14. For the nine measurement stations SCW, SWB, LEG, EUR, MPN, Ym6, K13, ELD and SON (see Fig. 3), the relative significant wave height was calculated from the results of the set 1 and set 2 computations. Figure 13 presents $\delta H_{m0}/H_{m0,\tau}$ against $\delta U_{10}/U_{10,\tau}$ for all instances

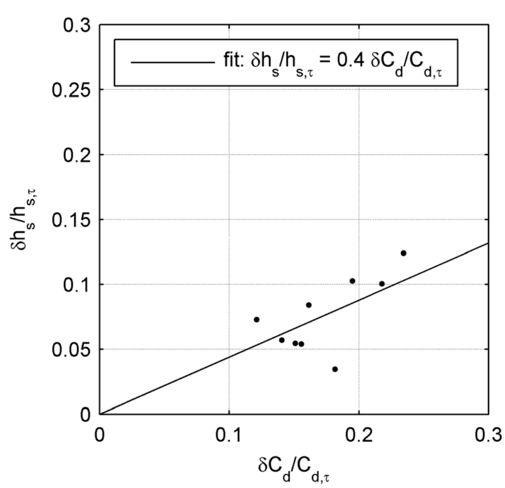

Fig. 10 The response of WAQUA in relative skew surge ($h_s/h_{s,\tau}$) is shown against the relative difference in drag coefficients $\delta C_d/C_{d,\tau}$ between HARMONIE and WAQUA for all instances where the surge S>1 m for the six coastal stations Vli, HvH, IJm, Hel, Harl and Del

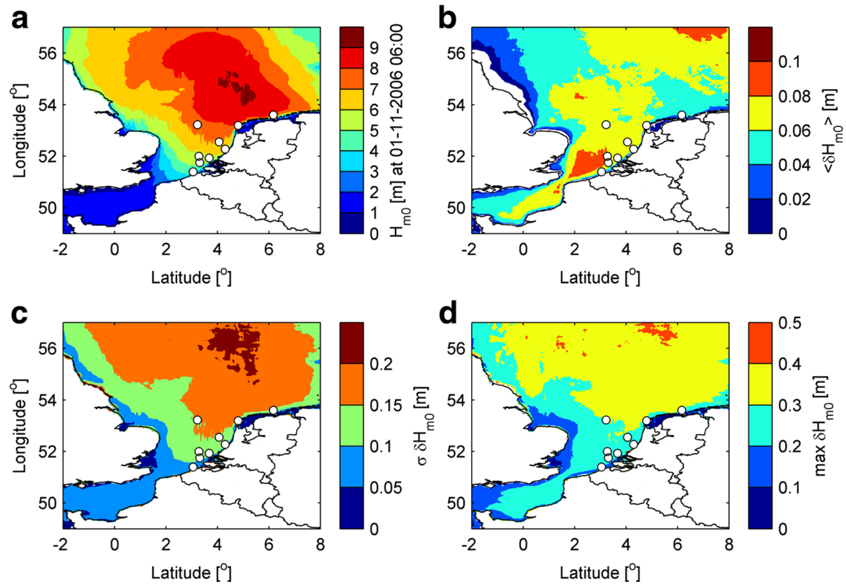

Fig. 11 **a** The significant wave height distribution for set 2 at the wave height peak at K13 on 1 November 2006, 06:00 is shown. **b** The mean difference of the significant wave height of set 1 and set 2 $<\delta H_{m0}>=<H_{m0,U}-H_{m0,\tau}>$. **c** The standard deviation σ for $\delta H_{m0}=H_{m0.U}-H_{m0,\tau}$. **d** Maximum difference for $\delta H_{m0}=H_{m0,U}-H_{m0,\tau}$

where $U_{10}>10$ m/s. A clear relation is observed between the relative wind velocity and the relative wave height; the response of $\delta H_{m0}/H_{m0,\tau}$ is double the relative difference in wind velocity for part of the data. However, for a cluster of data with ratios of $\delta U_{10}/U_{10,\tau}$ smaller than ca. 0.05, a smaller response in significant wave height is observed. These findings make sense bearing in mind that for fully developed seas, H_{m0} is proportional to $U_{10}{}^2$ and in other situations the proportionality varies from linear to quadratic with the wind speed (Janssen 2004). Therefore, $\delta H_{m0}/H_{m0,\tau}$ should vary between $\delta U_{10}/U_{10,\tau}$ and $2\delta U_{10}/U_{10,\tau}$.

Figure 14 shows the response of $\delta H_{m0}/H_{m0,\tau}$ against $\delta C_d/C_{d,\tau}$ for all instances where $U_{10}>10$ m/s. Again, a

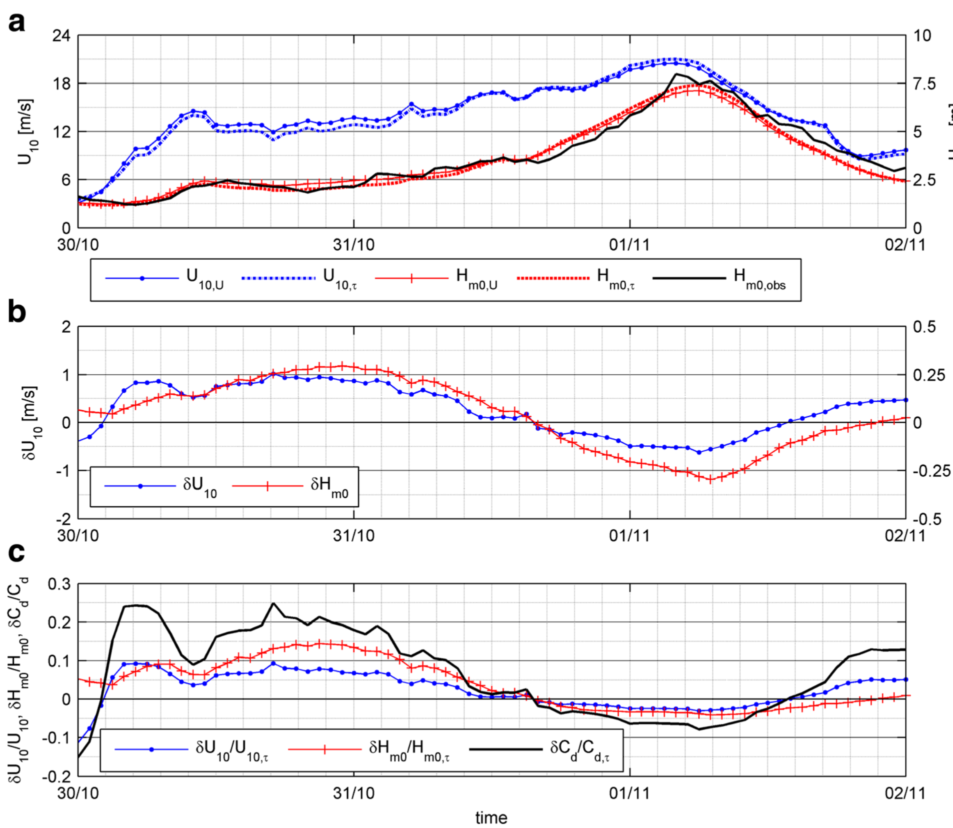

Fig. 12 Difference in significant wave height H_{m0} compared to difference in wind velocity and wind drag at K13. **a** The computed U_{10} and H_{m0} for set 1 and set 2 and the observed H_{m0}. **b** The absolute difference between set 1 and set 2 for U_{10} and H_{m0}. **c** The relative difference between set 1 and set 2 for U_{10}, H_{m0} and C_d

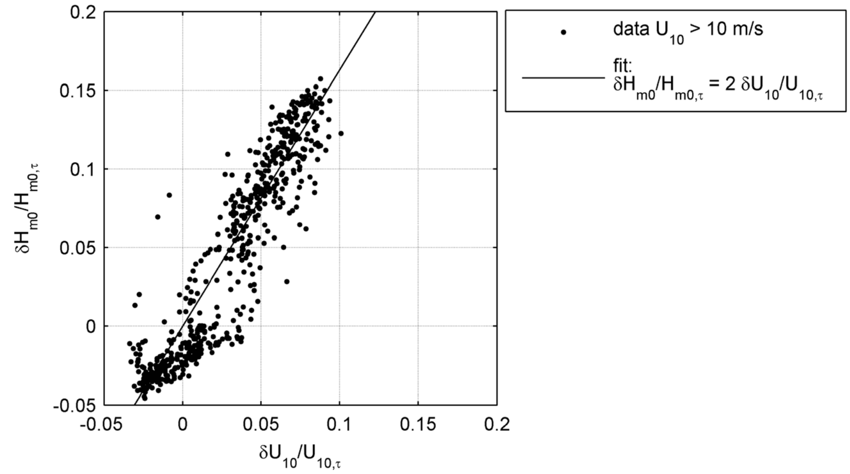

Fig. 13 The response of SWAN in relative significant wave height ($\delta H_{m0}/H_{m0,\tau}$) is shown against the relative difference in wind velocity $\delta U_{10}/U_{10,\tau}$ between HARMONIE and SWAN for all instances where U_{10}>10 m/s for the nine measurement stations SCW, SWB, LEG, EUR, MPN, Ym6, K13, ELD and SON

relation is found between $\delta H_{m0}/H_{m0,\tau}$ and $\delta C_d/C_{d,\tau}$, which is for part of the data

$$\frac{\delta H_{m0}}{H_{m0,\tau}} = 0.6\frac{\delta C_{d10}}{C_{d10,\tau}}.$$

This means that the response of waves is comparable to differences in drag coefficient with the response of surges. As was observed in the previous figure, the response is smaller for some data ($\delta C_d/C_{d,\tau}$ ratios<0.1).

5 Discussion and recommendations

Our study results show large differences between the waves and water levels computed with surface stress input and wind velocity input. The case study shows absolute differences of up to approximately 18 cm between the surge computations with surface stress input and wind velocity input. The relative response of the skew surge to differences in drag is approximately 40 % (60 % for surge). For the wave computations, the difference between the wave computations with surface stress input and wind velocity input is typically 20–30 cm in the coastal regions of The Netherlands. With 60 %, the relative response of the waves is even higher than the response in skew surge to differences in drag, but comparable to the response in surge. When comparing the surge, respectively wave computations to the measurements, we find that differences between observed and computed surges, respectively waves are larger than the differences due to inconsistent use of wind drag. However, using a consistent wind drag between the models can contribute to a proper identification of errors in the drag formulation and more accurate predictions of the surges and waves. We therefore would like to plea for the use of a consistent drag relation in meteorological, hydrodynamic and wave models.

With more complicated formulations of the wind drag in atmospheric models (e.g., ECUME relation in HARMONIE), it becomes increasingly difficult for modellers to use a

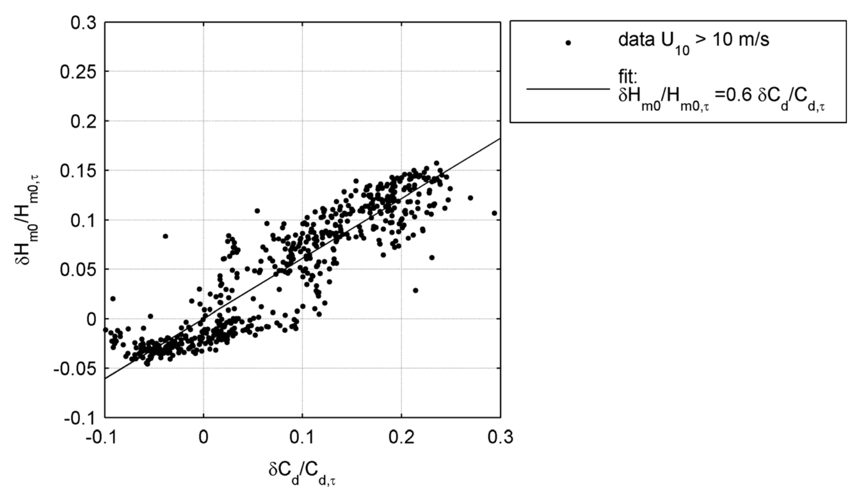

Fig. 14 The response of SWAN in relative significant wave height ($\delta H_{m0}/H_{m0,\tau}$) is shown against the relative difference in drag coefficients $\delta C_d/C_{d,\tau}$ between HARMONIE and SWAN for all instances where U_{10}>10 m/s for the nine measurement stations SCW, SWB, LEG, EUR, MPN, Ym6, K13, ELD and SON

consistent drag relation in the hydrodynamic models. The following options can be considered:

1. The easiest option is to make an approximation of the drag formulation (in terms of the Charnock parameter) and use this instead. For a model like WAQUA, where the Charnock formulation is implemented, this option is feasible; however, for a model like SWAN, this is not possible as no Charnock formulation is implemented in SWAN.
2. Ideally, one should directly use the surface stress, which is normally one of the outputs from an atmospheric model, avoiding therefore extra approximations. However, the problem with surface stress is that it offers a less intuitive interpretation than the wind velocity. Furthermore, the option to use the surface stress directly as a model input should be implemented in the model and this is not always the case.
3. Our suggestion is to use the so-called pseudo-wind, which is a translation of the surface stress provided by an atmospheric model to a 10-m wind speed using a reference drag relation and a reference air density. The modeller should subsequently use this reference drag relation and reference air density in his hydrodynamic model settings. The results of the pseudo-wind computations are the same as those of the stress computation. The use of a pseudo-wind ascertains that the model is fed with the stress as computed by the atmospheric model, while keeping the more intuitive interpretation of wind over stress.

The pseudo-wind solves the problem of inconsistencies in the drag relation between models. Even so, in our case study, we assume that the drag relation used in the considered atmospheric model is valid. This is not necessarily true, as a large uncertainty still exists in the magnitude of the drag coefficient, especially for extreme wind velocities. This uncertainty in the magnitude of the drag coefficient also influences the accuracy of the surface stress in the atmospheric model. Therefore, more measurements of the air-sea interface, especially during high wind speeds, are needed to improve the prediction of the drag coefficient.

Finally, when the wind drag is modelled, the influence of the sea surface and many related parameters is usually not taken into account. In our opinion, a proper modelling of the drag between air and sea can only be achieved if hydrodynamic, wave and atmospheric models are coupled.

Acknowledgments The research presented here is part of the WTI 2017 project ('Research and development of safety assessment tools of Dutch flood defences'), commissioned by the department WVL of Rijkswaterstaat in The Netherlands.

References

Baas P, Bosveld FC and Burgers G (2015) The impact of atmospheric stability on the near-surface wind over sea in storm conditions. Wind Energy. doi:10.1002/we.1825 DOI:10.1002/we.1825#Link to external resource: 10.1002/we.1825.

Babanin AV, Makin VK (2008) Effects of wind trend and gustiness on the sea drag: Lake George study. J Geophys Res 113(C2):2156–2202. doi:10.1029/2007JC004233

Booij N, Ris RC, Holthuijsen LH (1999) A third-generation wave model for coastal regions, part I, model description and validation. J Geophys Res 104(C4):7649–7666

Charnock H (1955) Wind stress on a water surface. Q J Roy Meteorol Soc 81:639–640

Dee DP et al (2011) The ERA-Interim reanalysis: configuration and performance of the data assimilation system. Q J Roy Meteorol Soc 137(656):553–597. doi:10.1002/qj.828

Gerritsen H, De Vries JW, Philippart M (1995) The Dutch continental shelf model. In: Lynch DR, Davies AM (eds) Quantitative skill assessment for coastal ocean models, vol 47. American Geophysical Union, Washington DC, pp 425–467

Janssen PAEM (2004) The interaction of ocean waves and wind. Cambridge University Press, Cambridge

Janssen PAEM, Doyle JD, Bidlot J, Hansen B, Isaksen L, Viterbo P (2002) Impact and feedback of ocean waves on the atmosphere. In Atmosphere-Ocean Interactions. In: Perrie W (ed) Advances in fluid mechanics, 33, vol 1. WIT Press, Boston, Massachusetts, pp 155–197

Makin VK (2004) A note on drag of the sea surface at hurricane winds. Bound-Lay Meteorol 115(1):169–176. doi:10.1007/s10546-004-3647-x

Muller H, Pineau-Guillou L, Idier D, Ardhuin F (2014) Atmospheric storm surge modeling methodology along the French (Atlantic and English Channel) coast. Ocean Dyn 64(11):1671–1692. doi:10.1007/s10236-014-0771-0

Powell MD, Vickery PJ, Reinhold TA (2003) Reduced drag coefficient for high wind speeds in tropical cyclones. Nature 422(6929):279–283

Seity Y, Brousseau P, Malardel S, Hello G, Bénard P, Bouttier F, Lac C, Masson V (2011) The AROME-France convective-scale operational model. Mon Weather Rev 139:976–991. doi:10.1175/2010MWR3425.1

Vatvani D, Zweers NC, Van Ormondt M, Smale AJ, De Vries H, Makin VK (2012) Storm surge and wave simulations in the Gulf of Mexico using a consistent drag relation for atmospheric and storm surge models. Nat Hazards Earth Syst Sci 12:2399–2410

Weill A, Eymard L, Caniaux G, Hauser D, Planton S, Dupuis H, Brut A, Guerin C, Nacass P, Butet A, Cloche S, Pedreros R, Durand P, Bourras D, Goirdani H, Lachaud G, Bouhours G (2003) Toward a better determination of turbulent air-sea fluxes from several experiments. J Climate 16:600–618

Wu J (1982) Wind-stress coefficients over sea surface from breeze to hurricane. J Geophys Res 87(C12):9704–9706. doi:10.1029/JC087iC12p09704

Zijl F, Verlaan M, Gerritsen H (2013) Improved water-level forecasting for the Northwest European Shelf and North Sea through direct modelling of tide, surge and non-linear interaction. Ocean Dyn 68: 823–847. doi:10.1007/s10236-013-0624-2

Zijlema M, Van Vledder GP, Holthuijsen LH (2012) Bottom friction and wind drag for wave models. Coast Eng 65:19–26

Zweers NC, Makin VK, De Vries JW, Burgers G (2011) On the influence of changes in the drag relation on surface wind speeds and storm surge forecasts. Nat Hazards 62(2):207–219. doi:10.1007/s11069-011-9989-z